This is a “preproof” accepted article for *Clay Minerals*.

This version may be subject to change during the production process.

10.1180/clm.2025.2

The effect of different exchangeable cations on the CO_2 adsorption capacity of Laponite RD®

Minh Hoang Nguyen[1], Liva Dzene[1*], Simona Bennici[1]

[1]Institut de Science des Matériaux de Mulhouse CNRS UMR 7361, Université de Haute-Alsace, Université de Strasbourg, 3b rue Alfred Werner, 68093 Mulhouse CEDEX, France

***Correspondance : liva.dzene@uha.fr**

Abstract

Tri-octahedral clay minerals have a potential to be used as CO_2 sorbents for intermediate temperatures (200-400 °C) owing to their thermal stability in this temperature range. In this study, laponite RD®, a commercially synthesized hectorite (with Na^+ as exchangeable cation) was used to investigate its capacity of CO_2 adsorption at 200 °C and ambient pressure. Different cations such as Co^{2+}, Ni^{2+}, Mg^{2+} and Ca^{2+} were employed to exchange Na^+ with the aim to study their effect on the capacity of adsorbing CO_2. The commercial sample showed an adsorption capacity of 144 $\mu mol_{CO2}/g$. Most of other exchanged sample displayed a deficit in the quantity of CO_2 adsorbed. An exception was the Ca^{2+}saturated sample, which exhibited a better performance (163 $\mu mol_{CO2}/g$) compared to the Laponite RD®. Thus, with higher affinity towards CO_2, such sample could be a good candidate for CO_2 capture. For all samples, most of the CO_2 was desorbed, and the formation of carbonate bonds was not observed by FTIR spectroscopy suggesting that the CO_2 was mainly physisorbed.

https://doi.org/10.1180/clm.2025.2 Published online by Cambridge University Press

Keywords: CO_2 adsorption, Laponite, cation exchange

Introduction

The release of CO_2 and other greenhouse gases due to human activities have contributed to the increase of atmosphere's temperature and subsequent climate change (Chevallier *et al.*, 2023). To limit the CO_2 release in the atmosphere different strategies are being studied. Great efforts are devoted to develop CO_2 capture and storage (CCS) technologies (Bui *et al.*, 2018). In addition to CCS, CO_2 capture and utilization (CCU) is also being considered. The possibility to use CO_2 released from one industrial process to generate new chemicals in other process agrees well with circular economy principle. Thus, CCU technology development is also an attractive strategy in the effort to limit the CO_2 emissions. For example, CO_2 can be used to produce methane in a heterogeneous catalytic process called methanation or Sabatier reaction. Methane can be then used further as a fuel or as a feedstock for the production of chemicals. Sabatier reaction requires moderate temperature and pressure conditions (<400 °C, 1 bar), and CO_2 conversion is achieved in a presence of catalyst (Vogt *et al.*, 2019). Recently, integrated CCU (ICCU) technology has been proposed, where CO_2 is captured and then converted in a single fixed-bed reactor under isothermal conditions (Omodolor *et al.*, 2020). Such system is more economically viable than the two separate units, because it reduces the energy required for sorbent regeneration, CO_2 storage and transport. In such system, a dual functional material (DFM) can be used. DFM exhibit at the same time a considerable CO_2 capture capacity and favorable catalytic properties for CO_2 conversion. It means combining together a catalyst, which is sufficiently efficient for CO_2 conversion, and a supporting material, which exhibits relatively high CO_2 capture capacity.

In literature, layered double hydroxides (LDH) derived mixed oxides and MgO are reported as CO_2 sorbents for intermediate temperatures (200-400 °C) such as that corresponding to

https://doi.org/10.1180/clm.2025.2 Published online by Cambridge University Press

Sabatier reaction (Wang *et al.*, 2014). Although clay minerals have been investigated as sorbents of CO_2 at low temperatures (<200 °C), their CO_2 adsorption capacity has not yet been assessed at intermediate temperatures. Indeed, most of the CO_2 sorbents, which are efficient at low temperatures, loose their stability upon heating, *e.g.* amines and metal organic frameworks. Tri-octahedral (Mg-rich) clay minerals remain stable in the intermediate temperature range, and thus their CO_2 adsorption capacity should be evaluated and compared to that of LDH. The abundance and low cost of clay minerals make them an attractive CO_2 sorbent for industry even if their CO_2 adsorption capacity might be lower than other sorbents. This study investigated CO_2 adsorption on Laponite, tri-octahedral commercial clay with high surface (Christidis *et al.*, 2018) at 200 °C. The CO_2 adsorption is expected to decrease with the increase of temperature, thus the lowest limit, i.e. 200 °C was chosen to assess the potential of Laponite for being used in such process. The sample was modified by a simple cation exchange to assess the effect of different exchangeable cations on CO_2 sorption capacity.

Materials and Methods

Preparation of cation-exchanged samples. Different chloride solutions were prepared to saturate commercial hectorite Laponite RD® with different cations such as Mg^{2+}, Ca^{2+}, Co^{2+} and Ni^{2+}. Laponite RD® (BYK-Chemie GmbH, Germany), magnesium chloride hexahydrate, $MgCl_2.6H_2O$ (Sigma-Aldrich, ≥ 99.0 wt%), calcium chloride dihydrate, $CaCl_2.2H_2O$ (Sigma-Aldrich, ≥ 99.0 wt%), nickel chloride hexahydrate, $NiCl_2.6H_2O$ (Thermo Scientific, 99.3 wt%), cobalt chloride hexahydrate, $CoCl_2.6H_2O$ (Acros Organics, 98.0 wt%) and deionized water of 18 MΩ.cm (Aquadem, PF 210, Veolia Water Technologies) were used. The cation-exchange process consisted of saturating the material with a highly concentrated chloride solution. 2.00 g (Precision Series, Fisherbrand) of Laponite RD were impregnated with 30 mL of 1 M chloride solution containing the exchangeable cation in a centrifuge tube.

https://doi.org/10.1180/clm.2025.2 Published online by Cambridge University Press

The tube was then agitated for at least 7 h before centrifugation at 8000 rpm (9946×*g*) for 10 min to remove the liquid phase (Rotanta 460, Hettich Zentrifugen). This step was repeated two times. Then the solid phase was washed with deionized water to remove the excess of chloride anions which was verified by adding Ag^+ in the supernatant ($AgNO_3$, Fluka, 99.0 wt%). The final product was oven-dried at 60 °C for 2 days (oven ED 056, Binder).

Physicochemical characterization methods. The structural properties of the samples were investigated by X-ray Diffraction (XRD) using a PANalytical MPD X'Pert Pro diffractometer (Almelo, The Netherlands) equipped with a Pixcel real-time multiple strip detector and operating with an angular aperture of 3.347° 2θ in the 2 to 70° 2θ range, and using CuKα radiation with a 0.15418 nm wavelength. XRD patterns were taken at 22 °C with a step size of 0.013° 2θ and a time per step of 218 s with the total time for acquisition of 1 h 15 mins. The divergence slit, the anti-scatter slit, and the two Soller slits were 0.0625, 0.125, and 2.3°, respectively.

Chemical composition of samples was determined using a wavelength dispersion X-ray Fluorescence (XRF) spectrometer Zetium from PANalytical (Almelo, The Netherlands). XRF experiments were carried out on pellets constituted of 0.3 g of the sample, pressed at 4 tons for 2 minutes.

Thermogravimetric analysis (TGA) of the samples was performed using a Mettler-Toledo TGA/DSC1 LF1100 apparatus (Switzerland), in alumina sample holders, under air, with a flow rate of 100 ml/min from 30 to 1000 °C and a heating rate of 10 °C/min. An empty sample holder was recorded as a reference to correct the baseline deviation.

Fourier transform infrared spectroscopy (FTIR) measurements were conducted using an Equinox IFS 55 apparatus (Karlsruhe, Germany) equipped with a DTGS detector from Bruker. The samples were mixed with KBr at a weight ratio of 1:100 and pressed at 4 bar for

https://doi.org/10.1180/clm.2025.2 Published online by Cambridge University Press

2 min, followed by oven-heating at 200 °C. The spectrum obtained was the average of 200 scans with a resolution of 4 cm^{-1}. The spectrum was recorded with the software OPUS, which was also used to subtract CO_2 and H_2O contributions.

N_2 adsorption-desorption isotherms were obtained on a Micrometrics ASAP 2420 equipment at -196 °C (Norcross, GA, USA). Prior to analysis, the samples were degassed at 300 °C for 15 hours and then again for 2 hours in the measurement emplacement. The degassing vacuum was 10^{-6} bar. The Brunauer, Emmett, and Teller (BET) equation ($0.01< P/P_0<0.40$) was used to calculate the specific surface area (SSA). The data were analyzed by means of the software MicroActive 5.02.

CO_2 adsorption tests. The CO_2 adsorption capacity of the samples was measured with a Setaram Sensys thermogravimetry-differential scanning calorimetry (TG-DSC) apparatus (France). The samples (around 15 mg) were first dehydrated at 300 °C under pure N_2 flow (30 mL/min) then the temperature was decreased and stabilized to the adsorption temperature (200 °C) always under N_2 flow. Once the mass was stabilized, the gas was switched to CO_2 with a constant flow of 30 mL/min and maintained during the CO_2 sorption experiments (30 minutes) until complete saturation of the samples. Finally, the gas was switched back again to N_2 also for 30 minutes (**Figure 1**). The changes in mass were recorded in order to evaluate the CO_2 adsorption capacity of the materials. The pressure of gases during CO_2 adsorption experiments was 3 bar. The specification of gases used in the experiment were: CO_2 N45 (purity of 99.995% and impurities less than 50 ppm) provided by AirLiquid (France) and N_2 4.5 (purity % ≥ 99,995) provided by Linde (France). Each experiment was performed twice, and the variation between the experiments did not exceed 5%.

Figure 1. Temperature profile for CO_2 adsorption and desorption at 200 °C.

https://doi.org/10.1180/clm.2025.2 Published online by Cambridge University Press

Results and discussion

Characterization of the exchanged materials. All samples displayed a similar structure with characteristic diffraction peaks corresponding to tri-octahedral swelling clay minerals (**Figure 2**) (Brindley & Brown, 1982). The (00ℓ) reflections were almost absent suggesting disordered stacking and /or low crystallinity. The broad peaks corresponding to (hkl) planes confirmed that all samples had small coherent scattering domain size. The similarity in XRD traces between Laponite RD and the exchanged samples showed that the crystal structure of original material was not impacted by the exchange protocol. No other additional crystalline phase precipitation occurred.

Figure 2. Powder X-ray diffraction patterns of Laponite® saturated with different cations.

FTIR analysis confirmed that all peaks were similar between the samples indicating that the basic structure of Laponite was not altered during the exchange process (**Figure 3**). The absorption bands such as stretching of O–H at 3680 cm^{-1}, of Si–O at around 1010 cm^{-1}, the bending of O–H at 657 cm^{-1} and Si–O at 450 cm^{-1} could be observed, characteristic of hectorite (Ogawa *et al.*, 2008; Yuan *et al.*, 2008; Yang *et al.*, 2022). Despite of the drying the pellets at 200 °C before the analysis, the bands attributed to bound water at 3445 and 1637 cm^{-1} were still present, however, their intensity was not significant compared to other characteristic bands of the samples.

Figure 3. FTIR spectra of Laponite® saturated with different cations.

The chemical composition of the samples determined by XRF (**Table 1**) confirmed that the exchangeable Na^{+} present in Laponite RD was replaced by Ni^{2+}, Co^{2+}, Mg^{2+} and Ca^{2+}. No sodium was detected by XRF in the exchanged samples.

Table 1. Chemical composition of Laponite® saturated with different cations determined by XRF.

Element	**Laponite (%at)**	**Ni_Lap (%at)**	**Co_Lap (%at)**	**Mg_Lap (%at)**	**Ca_Lap (%at)**
O	59.83	55.75	54.88	49.04	48.43
Mg	14.15	14.19	14.26	18.57	16.98
Si	23.94	25.49	25.90	32.25	31.63
Ca					2.85
Ni		4.32			
Co			4.83		
Na	1.80				

The N_2 physisorption isotherms of the Laponite samples were collected to determine their specific surface area (**Figure 4**). According to the IUPAC classification (Thommes *et al.*, 2015), all sample isotherms were of type IVa and hysteresis loop of type H3, indicating the presence of a mesoporous network with lamellar particles and fissure structures (Chen *et al.*, 2013). The samples showed relatively high surface areas ranging from 377 to 408 m^2/g (**Table 2**) compared to other common clay minerals. For Na-montmorillonite the specific surface area was reported to be 23 m^2/g (Dogan *et al.*, 2006). Such high surface area of Laponite compared to natural sample was due to the synthetic origin, which was influenced

https://doi.org/10.1180/clm.2025.2 Published online by Cambridge University Press

by production process (smaller particle size, particular dispersion and drying techniques). An improved adsorption of CO_2 compared to other common clay minerals could then be expected due to the high contact area with CO_2 molecules. The cation exchange had insignificant effect on the surface area of the samples.

Figure 4. N_2 adsorption (filled symbols) / desorption (empty symbols) isotherms of Laponite® saturated with different cations.

Table 2. Specific surface area and the amount of CO_2 adsorbed / desorbed of Laponite® saturated with different cations.

	Laponite	**Ni_Lap**	**Co_Lap**	**Mg_Lap**	**Ca_Lap**
SSA (m^2/g)	377	386	405	408	389
CO_2 ads (µmol/g)	144	68	60	93	163
CO_2 des (µmol/g)	129	55	52	80	138

To evaluate the thermal stability of samples, TGA was performed and the profiles were recorded (**Figure 5**). All samples exhibited similar profiles with the first mass loss at around 100 °C of about 13-14 wt% related to the dehydration. The second mass loss at around 765 °C of about 4-5 wt% was related to the dehydroxylation of the materials to form the corresponding mixed oxides (Earnest, 1983a; b). In general, all samples had a thermal stability between 200 and 650 °C which is desirable for a potential application as CO_2 sorbent in dual functional materials.

https://doi.org/10.1180/clm.2025.2 Published online by Cambridge University Press

Figure 5. TG curve and its derivative of Laponite® saturated with different cations. For all samples, the TG profiles are shown on the left axes and the DTG profiles are shown on the right axes.

CO_2 adsorption tests. **Figure 6** illustrates the amount of CO_2 adsorbed and desorbed at 200 °C for Laponite and cation exchanged samples. The Laponite adsorbed 144 µmol CO_2 per gram. As the cations were exchanged, a significant change appeared in CO_2 adsorption capacity of the samples. The samples Co_Lap and Ni_Lap showed an adsorption capacity reduced to less than half (60-68 µmol/g) compared to the Laponite. Mg_Lap performed better than the previous two samples but still less CO_2 was adsorbed compared to Laponite. The only sample that surpassed Laponite was the Ca_Lap where 163 µmol CO_2/g were adsorbed (13% higher compared to the Laponite). These results showed that among the cations that were exchanged, Ca^{2+} proved to be the one that had the best affinity with CO_2 molecules.

Figure 6. Amount of CO_2 adsorbed/desorbed at 200 °C after a pre-treatment at 300 °C under N_2.

As it can be seen in **Table 2**, the CO_2 adsorption capacity was not correlated to the specific surface area (SSA) of samples. Ca_Lap sample had the highest amount of CO_2 adsorbed while it represented an average specific surface. Thus, the difference in CO_2 adsorption capacity of different materials was not due to the SSA but influenced by the affinity of different cations towards CO_2. It has to be noted that the SSA determined with N_2 physisorption represented only the external surface of the material as the N_2 molecules were not able to enter the

https://doi.org/10.1180/clm.2025.2 Published online by Cambridge University Press

interlayer space. However, the CO_2 adsorbed molecules could be potentially adsorbed not only on the external surface, but also on the interlayer surface due to the fact that the CO_2 molecules are much smaller in size. Sample characterization by XRD and FTIR showed that the structure of material remained the same, thus the type of sites on the surface would also be expected to remain the same, the only difference being the exchangeable cations. Therefore, we hypothesize that the difference in CO_2 adsorption among the samples was related to the basicity of the respective cations. Indeed, as CO_2 is considered a Lewis acid, it tends to react with the most "basic" cation among those present after exchange. The pKa values provide insight into the basicity of cations in solution, where a higher pKa indicates greater basicity. With a pKa of 12.70, the $Ca^{2+}_{aq}/CaOH^{+}_{aq}$ pair exhibits higher basicity compared to the corresponding pairs of Mg (pKa = 11.40), Ni (pKa = 9.86), and Co (pKa = 9.80). Consequently, Ca^{2+} demonstrates the strongest affinity for CO_2 molecules due to its superior basicity. Laponite sample contained Na^{+} and Mg^{2+} as exchangeable cations. For this reason, the adsorption of CO_2 for Laponite sample was higher than that of Mg_Lap sample, which did not contain Na^{+}, but only Mg^{2+}. The adsorbed amount of CO_2 was smaller for Ni_Lap and Co_Lap samples compared to Mg_Lap, Lap (Mg+Na) and Ca_Lap samples due to the smaller basicity of Ni^{2+} and Co^{2+} as compared to Mg^{2+}, Ca^{2+} and Na^{+}.

The CO_2 desorption was performed by switching the inlet gas back to N_2 during 30 minutes. As shown in **Figure 6**, all samples desorbed 80-90% of the amount CO_2 adsorbed. These CO_2 molecules could be then expected to be as physiosorbed. The remaining 10-20% of CO_2 molecules could either be trapped within the porous structure or bonded chemically with the cations to form the corresponding carbonates. A FTIR analysis was performed on the Ca_Lap sample after it underwent the CO_2 adsorption-desorption test. A comparison between the same sample before and after CO_2 test is shown in **Figure 7**. It can be seen that main band corresponding to carbonate at 1460 cm^{-1} (Munawaroh *et al.*, 2019) was not observed.

https://doi.org/10.1180/clm.2025.2 Published online by Cambridge University Press

Calcium carbonate has two additional bands which are less intense at 880 cm^{-1}, and 712 cm^{-1}. A small change was observed for Ca_Lap sample after CO_2 adsorption around 800 cm^{-1}, but the absence of the most intense carbonate band suggested that there were no carbonates formed.

Figure 7. FTIR spectra of Ca_Lap before (black line) and after the CO_2 adsorption test (red line).

CO_2 gas phase band values are 2349 and 667 cm^{-1} respectively, but no band was observed around 2349 cm^{-1} in our study, and the band at 667 cm^{-1} overlapped with the strong band of O-H bending in material structure.

The materials studied in this paper were compared to other potential materials for CO_2 adsorption (**Table 3**). For intermediate temperatures (200-400 °C), two types of materials have been reported in the literature as CO_2 sorbents: mixed oxides derived from LDH and MgO.

https://doi.org/10.1180/clm.2025.2 Published online by Cambridge University Press

Table 3. Comparison of the CO_2 adsorption capacity at 200 °C/ 1 atm between Laponite cation-exchanged materials in this work and other materials from literature.

Material	Name	SSA (m^2/g)	CO_2 adsorbed (µmol/g)	Reference
Mg-Al 3:1 CO_3^{2-}	$Mg_3Al_1–CO_3$	154	720	(Gao *et al.*, 2013)
Mg-Al 3:1 CO_3^{2-} nano	LDH (IEP)	103	580	(Wang *et al.*, 2013)
Mg-Al 3:1 CO_3^{2-}	$Mg_3Al_1–CO_3$	239	530	(Wang *et al.*, 2011)
Mg-Al 3:1 CO_3^{2-}	Mg_3Al_1	239	410	(Wang *et al.*, 2010)
Mg-Fe 3:1 CO_3^{2-}	Mg_3Fe_1	255	462	(Wang *et al.*, 2010)
Li-Al 3:1 CO_3^{2-}	$LiAl_2–CO_3$	199	510	(Huang *et al.*, 2014)
Mg-Al 3:1 CO_3^{2-} C16	LDH-C16	348	910	(Qin *et al.*, 2017)
Mg-Al 3:1 CO_3^{2-} nano + K_2CO_3	K2CO3 – LDH (IEP)	n.d.	1210	(Wang *et al.*, 2013)
MgO	MgO		841	(Han *et al.*, 2012)
MgO-Al_2O_3 aerogel	5A5M		2977	(Han *et al.*, 2012)
MgO – biomass ash	MgO-RHA-20		4560	(Guo *et al.*, 2020)
Laponite RD	Lap	377	144	This work
Ca^{2+}-saturated Lap	Ca_Lap	389	163	This work

LDH with molar ratio Mg:Al of 3:1 and CO_3^{2-} as a charge compensating anion was reported to adsorb from 410 to 720 µmol/g of CO_2 (Table 3). Other charge compensating anions such as nitrates or chlorides decreased CO_2 adsorption capacity (Wang *et al.*, 2011). Replacement of Mg by Li or Al by Fe as well as the incorporation of organic acids slightly increased CO_2 adsorption capacity. The most efficient LDH modification was with K_2CO_3 where the material capacity to adsorb CO_2 was doubled from 600 to 1210 µmol/g. Further combination of alkali doping and organic acid-modification increased the LDH-based material adsorption

to 1930 µmol/g (Qin *et al.*, 2017). Other material reported for intermediate-temperature CO_2 capture was MgO. In a form of aerogel, it represented the CO_2 adsorption capacity much higher compared to that of LDH (2977 µmol/g). The modification with biomass ash increased materials CO_2 adsorption capacity even more (4560 µmol/g). Despite excellent CO_2 adsorption values, MgO was reported to present a problem of sintering which would decrease CO_2 adsorption capacity in long term (Zhao *et al.*, 2024).

Pristine Laponite tested in this study had approximately four times smaller CO_2 adsorption capacity compared to LDH and MgO. The modifications, such as cation exchange tested here, slightly increased CO_2 adsorption capacity, but the results were still not competitive with LDH.

In order to compare Ca_Lap with other clay minerals materials for which the CO_2 adsorption was performed at room temperature or lower, additional CO_2 adsorption experiments were performed. The pretreatment was done at 300 °C under N_2 flow as previously, but the adsorption of CO_2 was performed at 100 and 30 °C instead of 200 °C. As expected, the amount of CO_2 adsorbed increased. At 100 °C, Ca_Lap adsorbed 360 µmol/g and at 30 °C the adsorbed CO_2 value was 692 µmol/g. This value is similar or slightly higher compared to the values reported in the literature. Stevens *et al.* (2013) reported a CO_2 adsorption capacity of 490 µmol/g at 25 °C for K10 montmorillonite sample, and Azzouz *et al.* (2009) reported 685 µmol/g for Na montmorillonite.

Thus, Laponite had CO_2 adsorption capacity close to other smectites, but the amount of CO_2 adsorbed per g of material was significantly lower compared to other materials reported in intermediate temperatures (200-400 °C), e.g., LDH and MgO.

https://doi.org/10.1180/clm.2025.2 Published online by Cambridge University Press

Conclusion

In this work, we investigated the effect of the different cations exchanged with Na^+ of a Laponite RD® on CO_2 adsorption capacity. The samples were characterized throughout a series of physico-chemical methods which confirmed that the sample structure was not altered during the cation exchange process, and that the Na^+ was replaced by Co^{2+}, Ni^{2+}, Mg^{2+} and Ca^{2+}, respectively. With a CO_2 adsorption capacity at 200 °C of 163 µmol/g, the Ca^{2+}-saturated laponite (Ca_Lap) outperformed the other prepared samples and also was the only sample that outperformed the Laponite itself. This difference in CO_2 adsorption was related to the affinity of the cation with CO_2 and as Ca^{2+} had the best affinity, Ca_Lap adsorbed the most CO_2 among the samples. Furthermore, evidence from the infrared analysis after the CO_2 adsorption indicated that the CO_2 molecules were mostly physically adsorbed. High CO_2 adsorption capacity at 200 °C is one of the criteria for selecting materials for CO_2 capture and utilization process. Laponite had CO_2 adsorption capacity close to other similar clay minerals, but the amount of CO_2 adsorbed per g of material was significantly lower compared to other materials reported in intermediate temperatures (200-400 °C), e.g. LDH and MgO.

Credit author statement

Minh Hoang Nguyen: Data curation; Resources; Methodology; Investigation; Formal analysis; Visualization; Writing - original draft; Writing - review & editing. **Liva Dzene:** Conceptualization; Funding acquisition; Project administration; Supervision; Resources; Methodology; Formal analysis; Validation; Writing - review & editing. **Simona Bennici:** Conceptualization; Resources; Funding acquisition; Project administration; Supervision; Validation; Writing - review & editing. All authors have read and agreed to the published version of the manuscript.

Funding: This research was funded by the French National Research Agency, Project n° ANR-21-CE05-0023-02.

https://doi.org/10.1180/clm.2025.2 Published online by Cambridge University Press

Data Availability Statement: Data will be made available on request.

Acknowledgments: All physicochemical characterizations were performed on the IS2M technical platforms. The authors are very grateful to L. Michelin (XRD, XRF) and H. Nouali (ATG) for their contributions.

Conflicts of Interest: The authors declare no conflicts of interest.

References

Azzouz, A., Ursu, A.-V., Nistor, D., Sajin, T., Assaad, E. & Roy, R. (2009) TPD study of the reversible retention of carbon dioxide over montmorillonite intercalated with polyol dendrimers. *Thermochimica Acta*, **496**, 45–49.

Brindley, G.W. & Brown, G. (1982) *Crystal Structures of Clay Minerals and their X-ray Identification*. P. in.: Brookfield Pub Co, 495 pp.

Bui, M., Adjiman, C.S., Bardow, A., Anthony, E.J., Boston, A., Brown, S., Fennell, P.S., Fuss, S., Galindo, A., Hackett, L.A., Hallett, J.P., Herzog, H.J., Jackson, G., Kemper, J., Krevor, S., Maitland, G.C., Matuszewski, M., Metcalfe, I.S., Petit, C., Puxty, G., Reimer, J., Reiner, D.M., Rubin, E.S., Scott, S.A., Shah, N., Smit, B., Trusler, J.P.M., Webley, P., Wilcox, J. & Mac Dowell, N. (2018) Carbon capture and storage (CCS): The way forward. *Energy and Environmental Science*, **11**, 1062–1176.

Chen, D., Du, G., Zhu, Q. & Zhou, F. (2013) Synthesis and characterization of TiO2 pillared montmorillonites: Application for methylene blue degradation. *Journal of Colloid and Interface Science*, **409**, 151–157.

Chevallier, F., Crotwell, A., Gerbig, C., Jordan, A., Lan, X. & Loh, Z. (2023) The State of Greenhouse Gases in the Atmosphere Based on Global Observations through 2022. Pp. 1–11 in: *WMO Greenhouse Gas Bulletin*. Geneva.

https://doi.org/10.1180/clm.2025.2 Published online by Cambridge University Press

Christidis, G., Aldana, C., Chryssikos, G., Gionis, V., Kalo, H., Stöter, M., Breu, J. & Robert, J.-L. (2018) The Nature of Laponite: Pure Hectorite or a Mixture of Different Trioctahedral Phases? *Minerals*, **8**, 314.

Dogan, A.U., Dogan, M., Onal, M., Sarikaya, Y., Aburub, A. & Wurster, D.E. (2006) Baseline studies of the Clay Minerals Society source clays: specific surface area by the Brunauer Emmett Teller (BET) method. *Clays and Clay Minerals*, **54**, 62–66.

Earnest, C.M. (1983a) Thermal analysis of hectorite. Part I. Thermogravimetry. *Thermochimica Acta*, **63**, 277–289.

Earnest, C.M. (1983b) Thermal analysis of hectorite. Part II. Differential thermal analysis. *Thermochimica Acta*, **63**, 291–306.

Gao, Y., Zhang, Z., Wu, J., Yi, X., Zheng, A., Umar, A., O'Hare, D. & Wang, Q. (2013) Comprehensive investigation of CO2 adsorption on Mg–Al–CO3 LDH-derived mixed metal oxides. *Journal of Materials Chemistry A*, **1**, 12782. The Royal Society of Chemistry.

Guo, Y., Tan, C., Sun, J., Li, W., Zhang, J. & Zhao, C. (2020) Biomass ash stabilized MgO adsorbents for CO2 capture application. *Fuel*, **259**, 116298. Elsevier.

Han, K.K., Zhou, Y., Chun, Y. & Zhu, J.H. (2012) Efficient MgO-based mesoporous CO2 trapper and its performance at high temperature. *Journal of Hazardous Materials*, **203**–**204**, 341–347. Elsevier B.V.

Huang, L., Wang, J., Gao, Y., Qiao, Y., Zheng, Q., Guo, Z., Zhao, Y., O'Hare, D. & Wang, Q. (2014) Synthesis of LiAl 2 -layered double hydroxides for CO 2 capture over a wide temperature range. *Journal of Materials Chemistry A*, **2**, 18454–18462. Royal Society of Chemistry.

https://doi.org/10.1180/clm.2025.2 Published online by Cambridge University Press

Munawaroh, F., Muharrami, L.K., . T. & Arifin, Z. (2019) Synthesis and Characterization of Precipitated CaCO3 from Ankerite Prepared by Bubbling Method. *KnE Engineering*, **1**, 98.

Ogawa, M., Matsutomo, T. & Okada, T. (2008) Preparation of hectorite-like swelling silicate with controlled layer charge density. *Journal of the Ceramic Society of Japan*, **116**, 1309–1313.

Omodolor, I.S., Otor, H.O., Andonegui, J.A., Allen, B.J. & Alba-Rubio, A.C. (2020) Dual-Function Materials for CO2Capture and Conversion: A Review. *Industrial and Engineering Chemistry Research*, **59**, 17612–17631.

Qin, Q., Wang, J., Zhou, T., Zheng, Q., Huang, L., Zhang, Y., Lu, P., Umar, A., Louis, B. & Wang, Q. (2017) Impact of organic interlayer anions on the CO 2 adsorption performance of Mg-Al layered double hydroxides derived mixed oxides. *Journal of Energy Chemistry*, **26**, 346–353. Elsevier B.V.

Stevens, L., Williams, K., Han, W.Y., Drage, T., Snape, C., Wood, J. & Wang, J. (2013) Preparation and CO2 adsorption of diamine modified montmorillonite via exfoliation grafting route. *Chemical Engineering Journal*, **215**–**216**, 699–708. Elsevier B.V.

Thommes, M., Kaneko, K., Neimark, A. V, Olivier, J.P., Rodriguez-Reinoso, F., Rouquerol, J. & Sing, K.S.W. (2015) Physisorption of gases, with special reference to the evaluation of surface area and pore size distribution (IUPAC Technical Report). *Pure and Applied Chemistry*, **87**, 1051–1069. Pure and Applied Chemistry.

Vogt, C., Monai, M., Kramer, G.J. & Weckhuysen, B.M. (2019) The renaissance of the Sabatier reaction and its applications on Earth and in space. *Nature Catalysis*, **2**, 188–197.

https://doi.org/10.1180/clm.2025.2 Published online by Cambridge University Press

Wang, J., Huang, L., Yang, R., Zhang, Z., Wu, J., Gao, Y., Wang, Q., O'Hare, D. & Zhong, Z. (2014) Recent advances in solid sorbents for CO 2 capture and new development trends. *Energy Environ. Sci.*, **7**, 3478–3518. Royal Society of Chemistry.

Wang, Q., Tay, H.H., Ng, D.J.W., Chen, L., Liu, Y., Chang, J., Zhong, Z., Luo, J. & Borgna, A. (2010) The Effect of Trivalent Cations on the Performance of Mg-M-CO 3 Layered Double Hydroxides for High-Temperature CO 2 Capture. *ChemSusChem*, **3**, 965–973.

Wang, Q., Wu, Z., Tay, H.H., Chen, L., Liu, Y., Chang, J., Zhong, Z., Luo, J. & Borgna, A. (2011) High temperature adsorption of CO2 on Mg–Al hydrotalcite: Effect of the charge compensating anions and the synthesis pH. *Catalysis Today*, **164**, 198–203. Elsevier B.V.

Wang, Q., Gao, Y., Luo, J., Zhong, Z., Borgna, A., Guo, Z. & O'Hare, D. (2013) Synthesis of nano-sized spherical Mg3Al–CO3 layered double hydroxide as a high-temperature CO2 adsorbent. *RSC Advances*, **3**, 3414.

Yang, D., Chen, J., Hong, X., Cui, J. & Li, L. (2022) One-Pot Synthesis of TiO2/Hectorite Composite and Its Photocatalytic Degradation of Methylene Blue. *Catalysts*, **12**, 297.

Yuan, P., Annabi-Bergaya, F., Tao, Q., Fan, M., Liu, Z., Zhu, J., He, H. & Chen, T. (2008) A combined study by XRD, FTIR, TG and HRTEM on the structure of delaminated Fe-intercalated/pillared clay. *Journal of Colloid and Interface Science*, **324**, 142–149.

Zhao, C., Wang, L., Huang, L., Musyoka, N.M., Xue, T., Rabeah, J. & Wang, Q. (2024) Recent advances in intermediate-temperature CO2 capture: Materials, technologies and applications. *Journal of Energy Chemistry*, **90**, 435–452. Science Press.

https://doi.org/10.1180/clm.2025.2 Published online by Cambridge University Press

Figure 1:

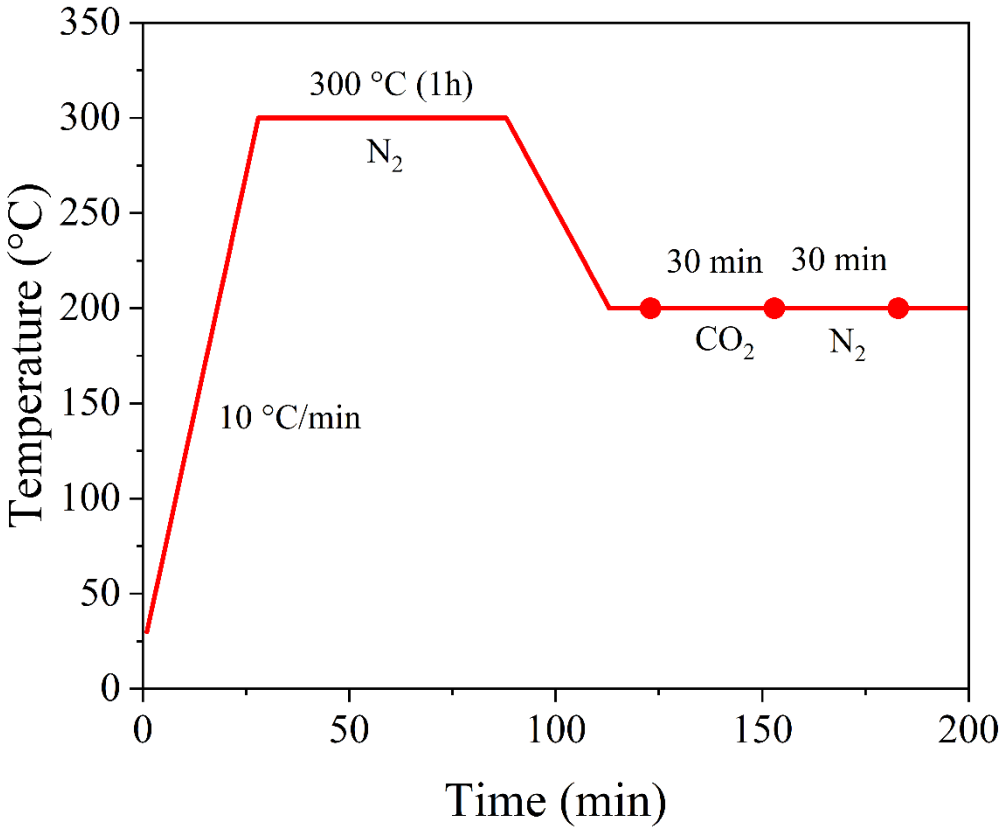

https://doi.org/10.1180/clm.2025.2 Published online by Cambridge University Press

Figure 2:

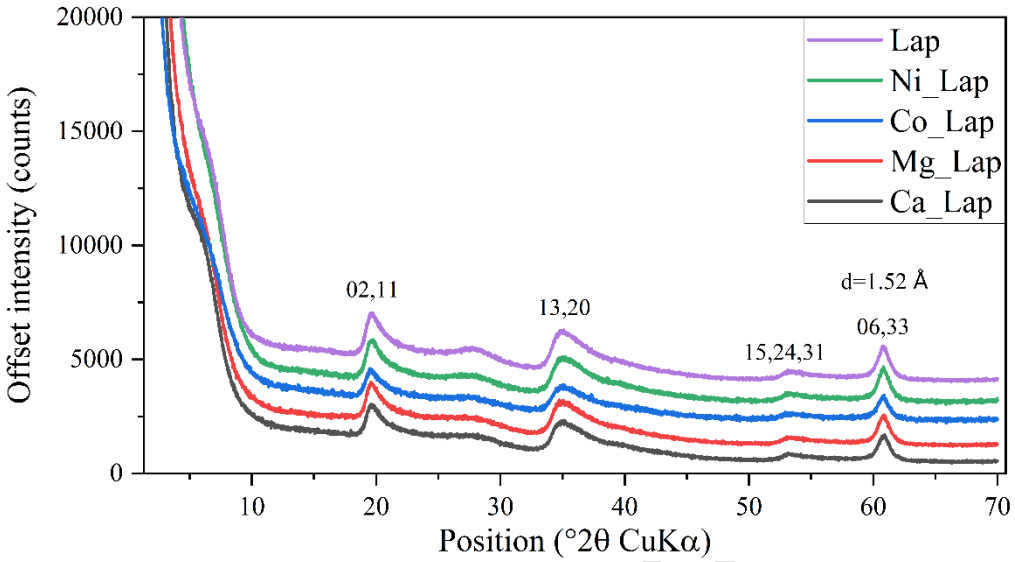

Figure 3:

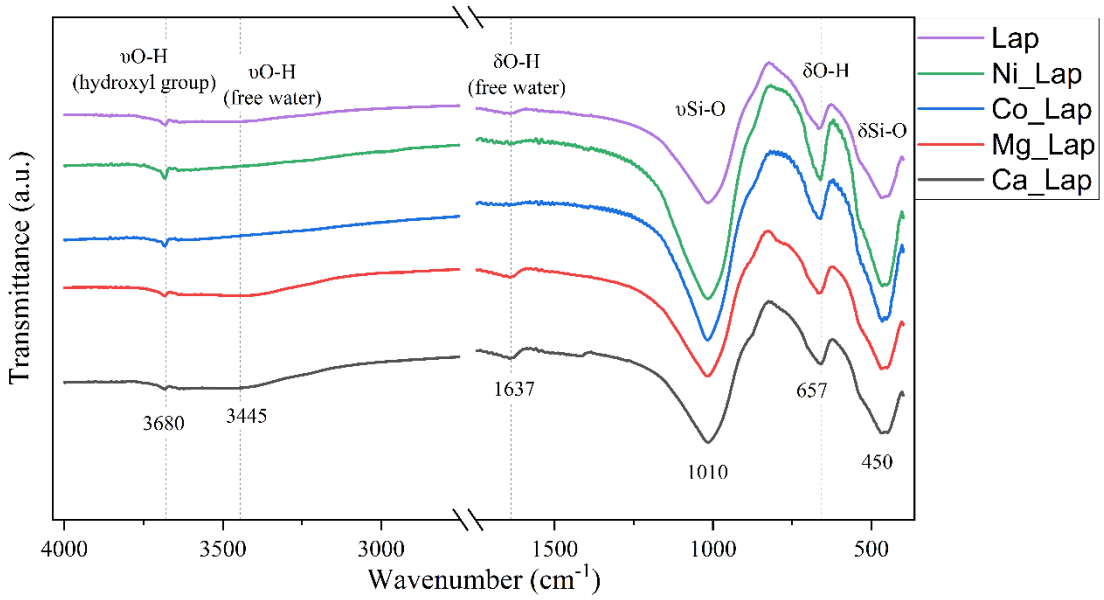

https://doi.org/10.1180/clm.2025.2 Published online by Cambridge University Press

Figure 4:

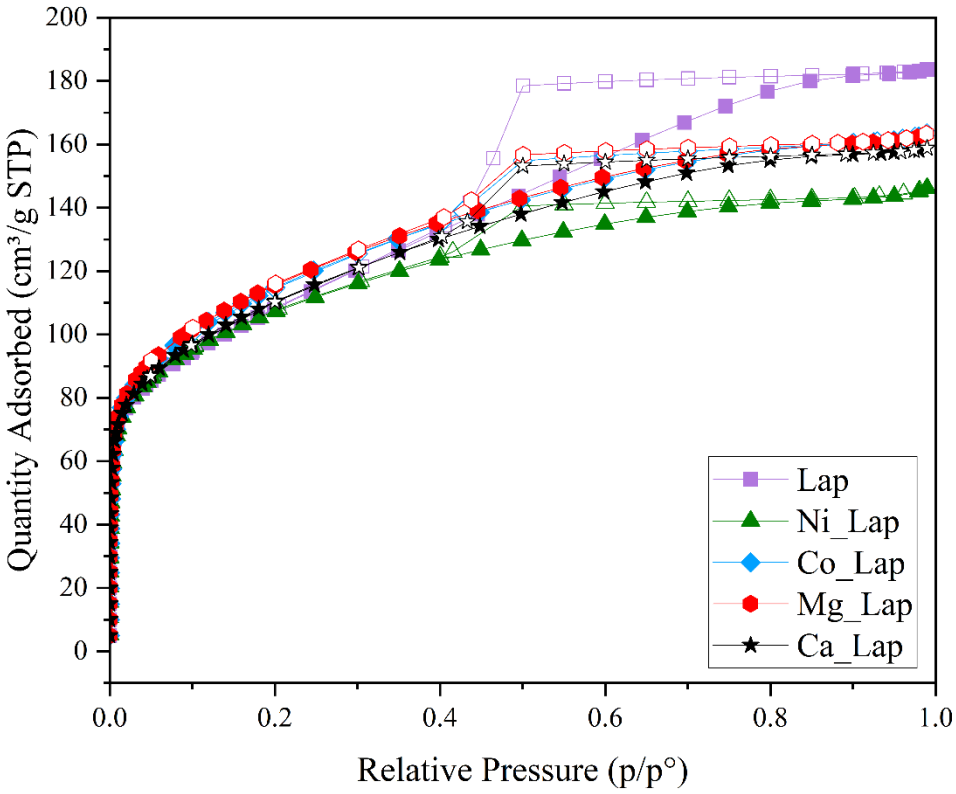

https://doi.org/10.1180/clm.2025.2 Published online by Cambridge University Press

Figure 5:

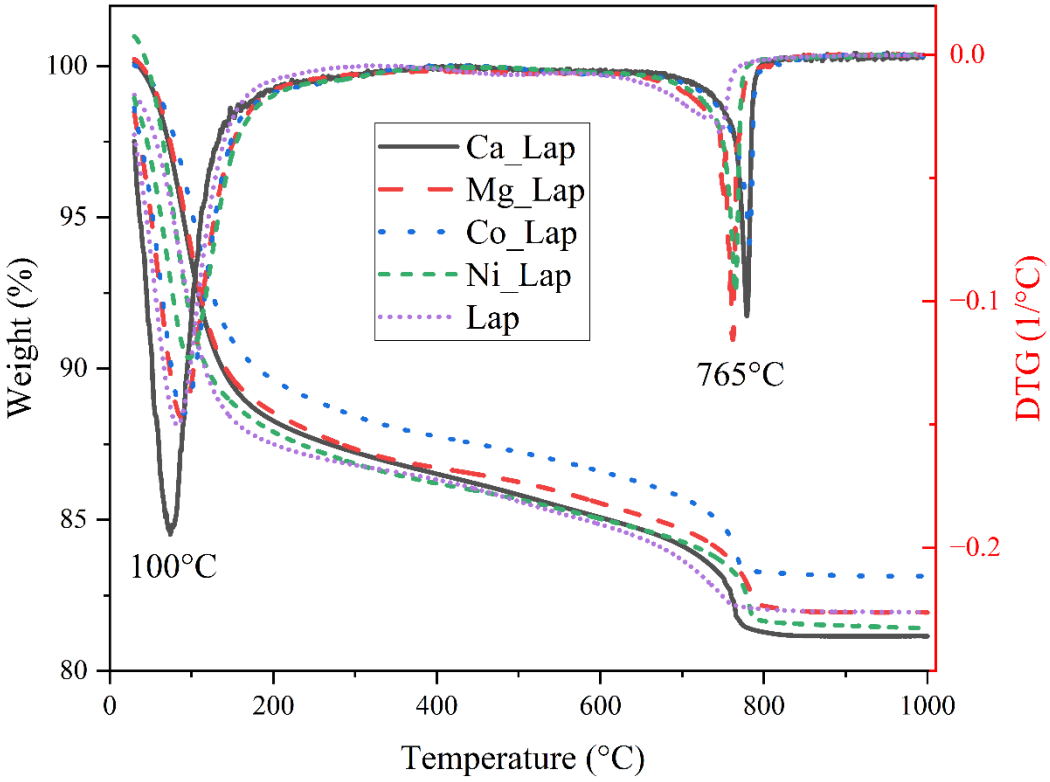

https://doi.org/10.1180/clm.2025.2 Published online by Cambridge University Press

Figure 6:

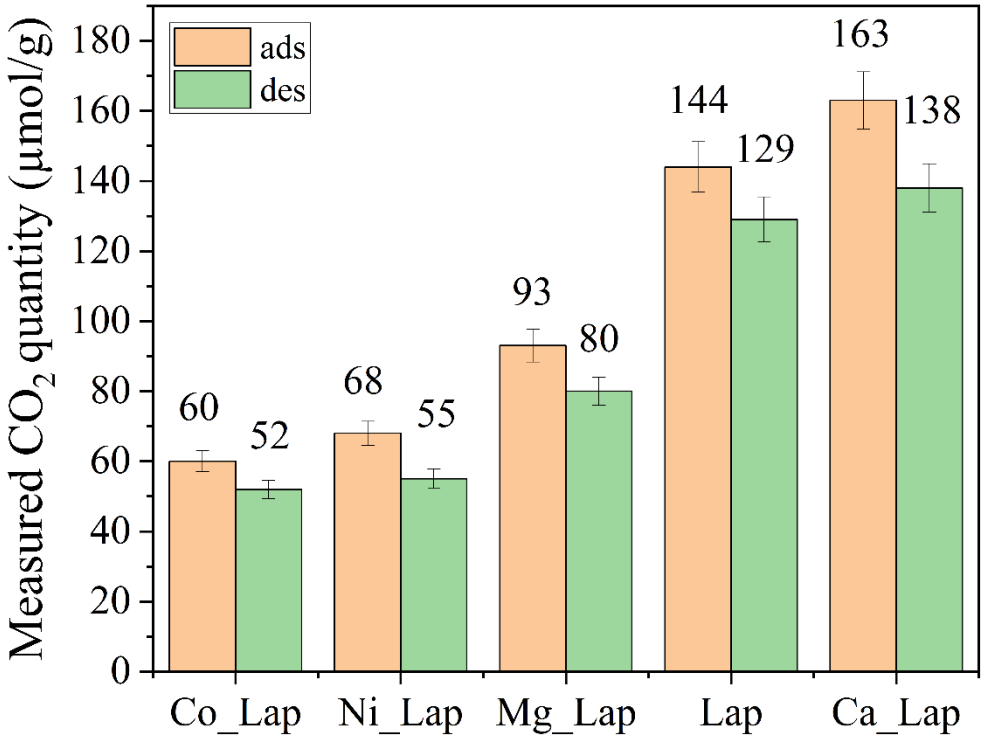

https://doi.org/10.1180/clm.2025.2 Published online by Cambridge University Press

Figure 7:

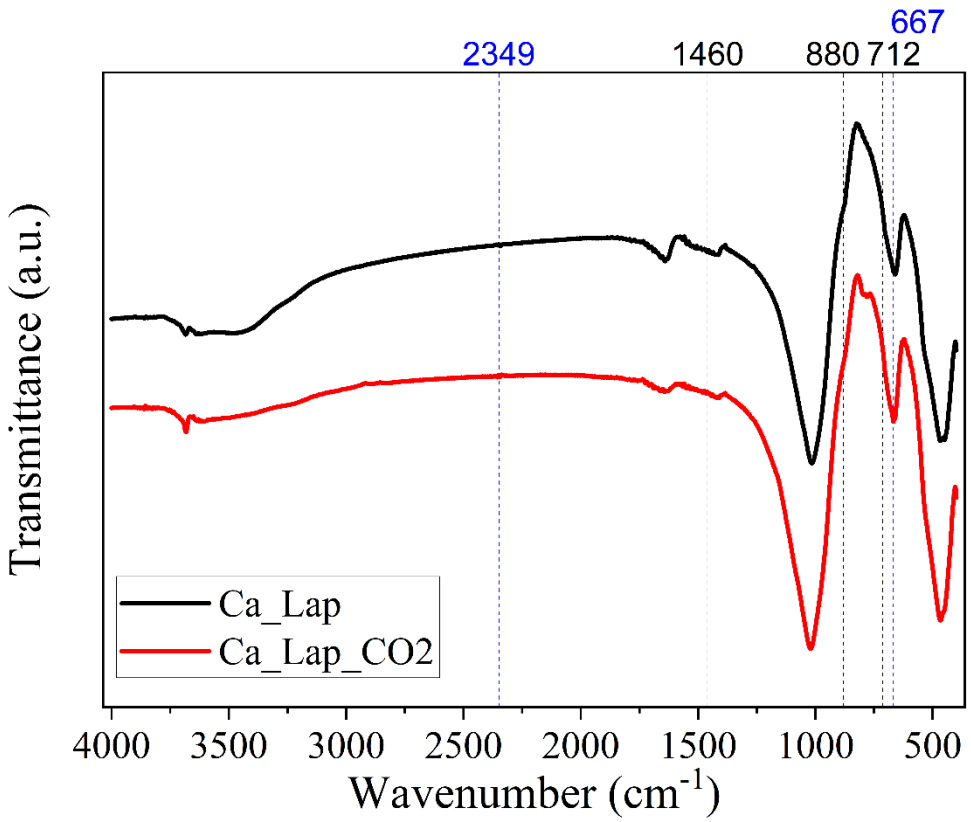

https://doi.org/10.1180/clm.2025.2 Published online by Cambridge University Press